

# Heat and mass transfer around an advancing penetrometer

ARTO M. YLINEN

Waterloo Centre for Groundwater Research, University of Waterloo, Waterloo, Ontario,  
Canada N2L 3G1

and

DEREK ELSWORTH

Department of Mineral Engineering, Pennsylvania State University, University Park, PA 16802, U.S.A.

(Received 17 January 1990 and in final form 3 July 1990)

**Abstract**—Measurement of the thermal field developed around a heated penetrometer tip is proposed as a method for determining the *in situ* flow and transport characteristics of unconsolidated saturated porous media. The purely diffusive thermal field developed around a static penetrometer is modified in the presence of penetration induced advective fluxes. The modification is conditioned by the advective thermal diffusivity and the elastic compressibility of the porous medium, enabling formation diffusivity to be evaluated where compressibility may be determined independently from the pressure transient record.

## 1. INTRODUCTION

OF CONSIDERABLE interest in predicting energy or mass migration within unconsolidated saturated porous media is the determination of the physical characteristics controlling transport. Measurement of the thermal field that develops around a heated penetrometer is proposed as a potential method of rapidly determining *in situ* parameters. This technique has been applied in determining the strength [1, 2], deformation [3, 4] and fluid consolidation characteristics [5-8] of soils with considerable success. Our application in the following is to explore the possibility of further applying the technique in determining permeabilities and porosities as they control the transport process.

In standard penetrometer testing, a conical  $60^\circ$  tip of  $1.78 \times 10^{-2}$  m radius is driven vertically into the porous medium, usually at a constant rate,  $U$ , of  $2 \times 10^{-2}$  m s $^{-1}$ . Pore fluid pressures are generated around the tip in response to displacement of the saturated porous medium as a result of tip insertion. The magnitude of the pore fluid pressures generated may be related to the strength characteristics [9, 10] of the soil but are also controlled by permeability magnitude [11]. The dissipation rate of tip pressures following arrest of the penetrometer may also be related to the coefficient of consolidation,  $C$ , of the porous medium [10] or analogous hydraulic diffusivity. Empirical correlations may further be used to determine permeability from hydraulic diffusivity [8, 11] but these techniques are extremely material specific. Unfortunately, knowledge of permeability or hydraulic diffusivity in the absence of a known

porosity gives no information on the advective transport characteristics of the porous medium. This additional information is, however, available if an advective transport mechanism, using heat as a tracer, is augmented at the penetrometer tip. Pore pressure gradients generated around the tip during penetration will advect heat from the thermal source and provide a thermal signature that may be measured along the advancing penetrometer shaft.

Traditional penetrometer testing of soft surficial soils is generally limited to the upper 30 m of the profile but is practical for any soil in which the penetrometer may be driven forward. The depth limit is therefore practically defined by the drive capacity of the propelling system. The proposed method is an alternative to sampling and laboratory testing enabling the rapid *in situ* determination of transport properties. Implicit in this method is the assumption that the advancing penetrometer does not drastically alter the *in situ* parameters that it attempts to measure. It is therefore critical that the bulk response around the advancing cone tip controls the transport and flow properties rather than the material at the penetrometer to soil interface, alone. The contribution of the soil volume surrounding the penetrometer has been illustrated to adequately reflect the fluid diffusive response [8] and it is assumed that a similar extension may be made in the determination of transport properties.

In addition to providing independent evaluation of consolidation parameters representing the porous medium, the thermal penetrometer is capable of providing transport parameters representative of thermal and mass transport behavior. As such, shallow sur-



capacity of the fluid saturated porous medium [ $\text{W s m}^{-3} \text{K}^{-1}$ ],  $T$  the temperature [K],  $t$  the time [s],  $\nabla$  the del operator [ $\text{m}^{-1}$ ] with the negative  $x$ -axis as the vector of penetration advance. This equation assumes the medium to be piecewise homogenous, isotropic and fully saturated by a single phase fluid. Additionally, the flux field driving the transport process must be steady and in most applications may be regarded as Darcian.

A steady state will propagate from the location of the moving source. The steady state develops only with reference to the moving reference frame of the penetrometer tip where a constant strength thermal source acts from the origin of the coordinate system. The steady condition develops as thermal energy is abstracted from around the source by the moving solid medium and flux field. This abstraction rate propagates outwards from the tip, varying spatially but becoming constant with time. To observe this in detail, it is useful to transform equation (1) into a Lagrangian form through substitution of the transformation

$$\zeta = x + Ut \quad (2)$$

where the  $y$  and  $z$  coordinates remain unchanged and a revised time parameter is substituted such that  $\tau = t$  where  $\tau$  is the time since initiation of penetration. In the revised coordinate system

$$\nabla_{(\zeta)} T = \nabla_{(x)} T \quad (3)$$

and

$$\frac{\partial T}{\partial t} = U \frac{\partial T}{\partial \zeta} + \frac{\partial T}{\partial \tau} \quad (4)$$

such that substitution into equation (1) yields

$$D_1 \nabla_{(\zeta)}^2 T - (\rho_1 c_1 \mathbf{q} + \rho_1 c_1 \mathbf{U}) \cdot \nabla_{(\zeta)} T + Q^* \delta(\zeta) = \rho_1 c_1 \frac{\partial T}{\partial \tau} \quad (5)$$

where  $\mathbf{U}$  is the vector [ $U, 0, 0$ ] $^T$ . When primary interest is in the thermal steady state around the penetrometer tip (measured relative to the moving frame of reference)  $\partial T / \partial \tau = 0$ , allowing the steady temperature distribution to be determined from subsidiary knowledge of the Darcian fluxes.

**2.1.1. Dimensionless parameters.** In describing thermal behavior it is convenient to define a minimum set of dimensionless parameters that control system performance. Thermal transfer away from the moving thermal source is most efficient when either the source moves through the medium at high velocity,  $U$ , or where the advective flux term,  $\mathbf{q}$ , dominates. Conversely, for constant source strength,  $Q^*$ , temperature build-up in the vicinity of the source is greatest where  $U \rightarrow 0$ ,  $\mathbf{q} \rightarrow \mathbf{0}$  and the system of equation (1) may be simplified to the spherically symmetric heat flow equation as

$$D_1 \frac{1}{r^2} \frac{\partial}{\partial r} \left( r^2 \frac{\partial T}{\partial r} \right) = \rho_1 c_1 \frac{\partial T}{\partial t} \quad (6)$$

where  $r$  is the radius of interest. Applying an outer boundary condition at infinity as

$$\lim_{r \rightarrow \infty} T(r) = T_\infty \quad \forall t. \quad (7)$$

The solution for equation (6) under conditions of constant thermal power input  $Q$  [W] distributed uniformly over the surface  $r = r_0$  and with homogenous initial temperature,  $T_\infty$ , is well known [12] as

$$T(r, t) = T_\infty + \frac{Q}{4\pi D_1 r} \left\{ \operatorname{erfc} \left[ \frac{r - r_0}{2(\kappa_1 t)^{1/2}} \right] - \exp \left[ \frac{r - r_0}{r_0} + \frac{\kappa_1 t}{r_0^2} \right] \cdot \operatorname{erfc} \left[ \frac{r - r_0}{2(\kappa_1 t)^{1/2}} + \frac{(\kappa_1 t)^{1/2}}{r_0} \right] \right\} \quad (r > r_0; t > 0) \quad (8)$$

where  $\kappa_1$  is the thermal diffusivity of the saturated system,  $\kappa_1 = D_1 / \rho_1 c_1$ . In the steady state as  $t \rightarrow \infty$  and  $1/t \rightarrow 0$  the asymptotic values of the complementary error function,  $\operatorname{erfc}(x)$ , yield

$$T(r, \infty) = T_\infty + \frac{Q}{4\pi D_1 r} \quad (r > r_0) \quad (9)$$

representing the maximum limiting value of equation (8) in time. The absolute maximum occurs at  $r = r_0$ . From this, dimensionless temperature,  $T_D(r, t)$ , may be usefully defined as

$$T_D(r, t) = \frac{4\pi D_1 r_0 (T(r, t) - T_\infty)}{Q} \quad (10)$$

with bounds  $0 \leq T_D(r, t) \leq 1$ . The steady form of equation (8) is correspondingly

$$T_D(r_D, \infty) = \frac{1}{r_D} \quad (11)$$

where  $r_D = r/r_0$  is a dimensionless radial ordinate and describes the  $1/r$  variation in temperature in the diffusive, static, steady state.

Although initially referenced to the static system, the dimensionless variables of temperature  $T_D(r, t)$  and ordinate  $r_D$  may be augmented by the parameters controlling the moving system. These are

$$x_D = \zeta / r_0 \quad (12)$$

$$t_D = \frac{D_1 \tau}{\rho_1 c_1 r_0^2} \quad (13)$$

$$\mathbf{q}_D = \frac{r_0}{2C} \mathbf{q} \quad (14)$$

and

$$U_D = \frac{r_0}{2C} \mathbf{U}. \quad (15)$$

They represent dimensionless quantities of distance  $x_D$ , time  $t_D$ , flux  $\mathbf{q}_D$ , and penetration rate  $U_D$ , where all parameters are as previously defined and  $C$  is the

coefficient of consolidation [ $\text{m}^2 \text{s}^{-1}$ ] of the porous medium. Accordingly the Lagrangian form of equation (5) is

$$\nabla_{\text{D}}^2 T_{\text{D}} - Pe \left\{ \frac{1}{c_{\text{sf}}} \frac{\mathbf{q}_{\text{D}}}{U_{\text{D}}} + \mathbf{x}^0 \right\} \cdot \nabla_{\text{D}} T_{\text{D}} + \frac{4\pi}{V_{\text{D}}} \Delta(x_{\text{D}}) = \frac{\partial T_{\text{D}}}{\partial t_{\text{D}}} \quad (16)$$

with the ratio of specific heat capacities of the porous medium and fluid given as  $c_{\text{sf}} = \rho_1 c_1 / \rho_f c_f$ , and the volume of heat generation defined as  $V_{\text{D}} = V/r_0^3$  where  $r_0$  is the effective radius of the source and  $V$  the source volume.  $\Delta$  corresponds to  $\delta$  for a finite volume source of volume  $V_{\text{D}}$ . Additionally,  $\mathbf{x}^0$  is the unit vector in the  $x$ -direction and the dimensionless Peclet number is defined as  $Pe = Ur_0/\kappa_1$ . Heat generation occurs within this volume such that

$$Q = Q^*V. \quad (17)$$

It is understood that  $V$  represents a fictitious parameter used in modeling to prevent a thermal singularity at the origin and as such does not represent any particular aspect of penetrometer or source geometry.

**2.1.2. Functional dependence.** The distribution of dimensionless temperatures around the advancing penetrometer is conditioned by the first two terms of equation (16). The first represents the diffusive component onto which is superimposed the influence of advective fluxes. The importance of the advective term is controlled by the parameter

$$\kappa_{\text{D}} = Pe \left\{ \frac{\mathbf{q}_{\text{D}}}{c_{\text{sf}} U_{\text{D}}} + \mathbf{x}^0 \right\} \quad (18)$$

which varies spatially around the penetrometer as a function of the fluid flux field,  $\mathbf{q}_{\text{D}}$ . The first part is a Peclet number representing the ratio of advective thermal flux to the diffusive flux. The second represents the skewness of the temperature distribution as influenced by penetration rate.

## 2.2. Mass transport equation

The steady flux distribution in the moving local coordinate system may be determined as [11]

$$p(x, r) = p^s + \frac{\mu}{k} \frac{Ur_0^2}{4R} \exp[-U(R-x)/2C] \quad (19)$$

where  $p(x, r)$  is the induced pressure change [Pa],  $p^s$  the static fluid pressure [Pa],  $k$  the permeability [ $\text{m}^2$ ],  $\mu$  the dynamic viscosity of fluid [Pa s],  $r_0$  the radius of the penetrometer,  $C$  the consolidation coefficient [ $\text{m}^2 \text{s}^{-1}$ ] and  $R = (x^2 + r^2)^{1/2}$ . Flux may be determined from Darcy's law where

$$\mathbf{q} = -\frac{k}{\mu} \nabla p \quad (20)$$

and substituting equation (19) gives in dimensional form

$$\mathbf{q} = \frac{Ur_0^2}{4} \left\{ \begin{array}{l} \left( \frac{U}{2CR} + \frac{1}{R^2} \right) \frac{x}{R} - \frac{U}{2CR} \\ \left( \frac{U}{2CR} + \frac{1}{R^2} \right) \frac{r}{R} \end{array} \right\} \times \exp[-U(R-x)/2C] \quad (21)$$

or in dimensionless representation

$$\mathbf{q}_{\text{D}} = \frac{U_{\text{D}}}{4R_{\text{D}}^2} \left\{ \begin{array}{l} U_{\text{D}}(x_{\text{D}} - R_{\text{D}}) + \frac{x_{\text{D}}}{R_{\text{D}}} \\ U_{\text{D}}r_{\text{D}} + \frac{r_{\text{D}}}{R_{\text{D}}} \end{array} \right\} \times \exp[-U_{\text{D}}(R_{\text{D}} - x_{\text{D}})] \quad (22)$$

which may be substituted directly into equation (16) in evaluating the distribution of dimensionless temperature in the vicinity of the penetrometer.

## 2.3. Numerical procedure

Pore pressures around the advancing penetrometer are developed from a moving center of dilation that represents the insertion of an amorously tipped or blunt cylinder. The tapered tip of the penetrometer is not explicitly represented. This approach has been found adequate in comparisons with actual penetrometer data in representing the pressure field [11].

The finite difference solution is sought to equation (16) subject to the associated flux conditions. The Cartesian form of the diffusion equation is transformed to an axisymmetric form enabling solution in the  $(x, r)$  coordinate system with positive  $x$  representing the distance behind the moving penetrometer tip. Node points have a single unknown of temperature and a logarithmic spatial distribution is used in the  $r$ -direction to maximize solution accuracy. The physical system is illustrated in Fig. 1(a) representing a heat source present in the vicinity of the tip of a moving penetrometer. The finite size thermal source is of radius  $r_0$  and nominal length  $2r_0$  and surrounded by an infinite porous medium. Heat generation is confined to the curved surface of this shell as a constant Neumann boundary condition, moving with velocity  $U$ . The finite form of the source distributes the resulting thermal flux over a series of adjacent elements (along the penetrometer length), most faithfully representing the anticipated true physical form of the source and reducing problems of numerical instability.

## 3. PENETROMETER BEHAVIOR

Primary interest is in the steady flow and heat transport behavior behind the advancing tip of the penetrometer as this is the extent of access for measuring temperatures in the porous medium. Of specific interest are the parameters that control the thermal transport processes and therefore exert a dominant influence on the resulting temperature field. These

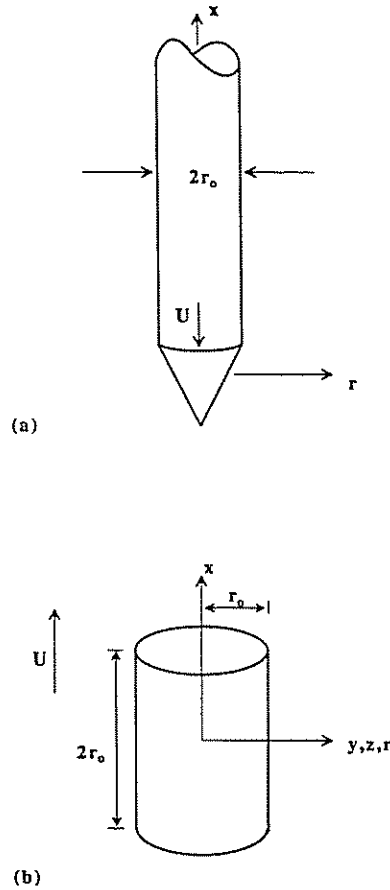


FIG. 1. Penetrator geometry showing (a) penetrator form and (b) system geometry with coordinate system fixed to cylindrical heat source shell. Heat source moves with velocity  $-U$  relative to the penetrated medium.

processes control the parameters that may sensibly be derived from field results.

3.1. Controlling parameters

In steady penetration, the spatial field of hydraulic flux,  $q_D$ , is a function of dimensionless penetration rate,  $U_D$ , only, as apparent from equation (22). For  $U_D \leq 10^0$  the pressure field is spherical and varies as  $1/R$  [11]. As  $U_D$  increases, the pressure field remains as  $1/x_D$  along the penetrator shaft ( $x_D > 0; r_D = 1$ ) but gradients to the side and ahead of the tip steepen considerably to yield an elongated bulb. For a single source geometry the thermal field is modified by the flux distribution,  $q_D$ , as evidenced in the dimensionless parameter

$$\kappa_D = Pe \left\{ \frac{q_D}{c_{st} U_D} + x^0 \right\} \tag{18}$$

in equation (16) where flux is a unique function of  $U_D$ . If advective transport is neglected ( $q_D = 0$ ), the thermal field is uniquely controlled by the reduced dimensionless quantity  $Pe = Ur_0/\kappa_1$  representing the

diffusive characteristics of the penetrated medium. The form of the resulting diffusive thermal field is identical to the diffusive pressure field that results from the moving dislocation. For  $Pe \leq 10^0$  the temperature field is spherical and exhibits a  $1/R_D$  distribution away from the tip. This response is a direct result of the spherical flux field that is exhibited for small penetration rates,  $U_D$ . At higher penetration velocities,  $Pe > 10^0$ , the thermal distribution loses spherical symmetry and becomes compressed both to the side and ahead of the penetrator. The temperature distribution varies as  $1/x_D$  along the  $x_D > 0$  axis for all  $Pe$  with only the absolute magnitude controlled by the thermal diffusivity. Consequently, where the thermal field is predominantly diffusive, the temperature distribution may be used to determine the thermal diffusivity of the penetrated medium, only. The unique variation of dimensionless temperature,  $T_D$ , along the shaft, illustrated in Fig. 2, indicates that the temperature field alone is not a discriminant for hydraulic parameters where thermal transport is purely diffusive. The slight mismatch between the two temperature distributions of Fig. 2 results from the slightly different geometric representations of the source. The  $1/x$  distribution represents a spherical source and the numerical model is a cylindrical source of 1 : 1 length to diameter ratio. As expected the two temperature distributions converge away from the location of the source.

Since  $T_D = 1/x_D$  for  $q_D = 0$ , any change to this distribution results from the influence of hydraulic flux as  $q_D \neq 0$  or alternatively,  $Pe \neq 0$ . Thus, any deviation from the inverse radial distribution implies the presence of a significant hydraulic flux constituting the first term of  $\kappa_D$ . The first term of  $\kappa_D$  may be rewritten by substituting equations (14) and (15), together with  $Pe = Ur_0/\kappa_1$  and  $c_{st} = \rho_r c_r / \rho_c c_c$  into equation (18). This results in

$$\kappa_D = \frac{\rho_r c_r}{D_1} r_0 q + Pe x^0 \tag{23}$$

where  $\rho_r c_r / D_1$  is the thermal diffusivity component controlled by the fluid filled porosity,  $r_0$  the source

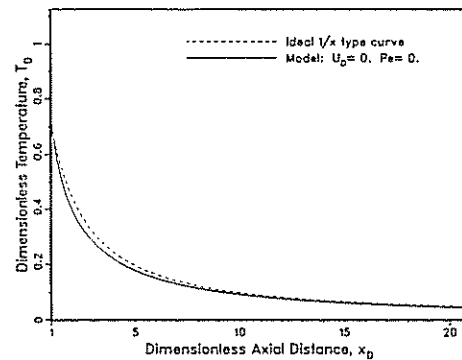


FIG. 2. Limiting radial temperature distribution for purely diffusive transport or static thermal source  $T_D = 1/x_D$ .

radius and  $\mathbf{q}$  the spatially varying hydraulic flux field. The thermal diffusivity may be determined within reasonable bounds, excepting the porosity component, leaving  $\mathbf{q}$  as the dominant unknown. The flux field (see equation (21)) is controlled by a known or defined penetration rate,  $U$  (as embodied in  $Pe$ ), and an unknown dimensionless penetration rate,  $U_D$ , incorporating the consolidation coefficient,  $C$ . This implies that  $U_D$  may be determined uniquely from the thermal signature measured along the shaft, and consequently the magnitude of the consolidation coefficient evaluated. This prognosis requires that the induced hydraulic flux field is sufficiently important that measurable deviations in  $T_D$  may be recorded. Suitable ranges of  $U_D$  are examined in the following as a function of  $Pe$  and  $U_D$ .

### 3.2. Parametric results

Modification of the axial temperature distribution along the penetrometer shaft from the form  $T_D = 1/x_D$  (Fig. 2) is controlled by the two partially dependent parameters of Peclet number  $Pe = Ur_0/\kappa_1$ , and dimensionless penetration rate,  $U_D = Ur_0/2C$ . The results are most conveniently viewed for a variety of dimensionless penetration rates, representing variable consolidation coefficients, at a constant real penetration rate.

Thus, for reasonable thermal characteristics of the penetrated medium,  $\kappa_1$ , and at constant prescribed penetration rate,  $U$ , the Peclet number will remain constant. The diffusive thermal characteristics embodied in  $\kappa_1$  are relatively insensitive to the permeability or elastic modulus to which consolidation coefficient,  $C$ , is directly proportional. Therefore, varying the consolidation coefficient,  $C$ , changes the dimensionless penetration rate,  $U_D$ , without materially altering  $Pe$ . Figure 3 illustrates results for penetration of a standard cone penetrometer of nominal radius  $r_0 = 1.78 \times 10^{-2}$  m and penetration rate  $U = 2 \times 10^{-2}$  m s $^{-1}$  ( $Pe = 625$ ). The axial temperature distribution is flattened over the case of purely diffusive flow as a direct result of the hydraulic flux. Advecting fluid allows rapid thermal dissipation

from close to the tip to the far field. Consequently, dimensionless temperatures are low ( $T_D \leq 0.07$ ) for the full range of dimensionless penetration rate magnitudes. As the consolidation coefficient magnitude decreases (representing a decrease in fluid permeability or decrease in elastic modulus of the porous medium) the axial temperature distribution initially increases from the threshold magnitude at  $U_D < 10^{-2}$  and then falls to the limiting lower value representing  $U_D \geq 10^2$ . The sensitivity range to variations in  $U_D$ , where the steady temperature profile is visibly affected, spans four orders of magnitude. The lower temperature distribution results from the high pore pressure gradients generated along the penetrometer shaft [11] that efficiently advect heat into the surrounding medium.

As real penetration rate is reduced an order of magnitude ( $U = 2 \times 10^{-3}$  m s $^{-1}$ ,  $Pe = 62.5$ ) the magnitude of attainable shaft temperatures increase, as illustrated in Fig. 4. As dimensionless penetration rate increases above the threshold of  $U_D \approx 1$  the temperature distribution decreases to a lower threshold for  $U_D \geq 10$ . Although the range of dimensionless temperatures,  $T_D$ , has increased, the sensitivity to the penetration rate,  $U_D$ , has been restricted to the range  $10^{-2} \leq U_D < 10^1$ . The sensitivity span has been decreased to three orders of magnitude in this instance. Further decreasing real penetration rate or the shaft radius by an order of magnitude ( $Pe = 6.25$ ), as illustrated in Fig. 5, elicits a similar pattern of response but with a sensitivity span of only a single order of magnitude. Decreasing real penetration rate allows the steady temperature distribution to successively approach the diffusive transport distribution of  $T_D = 1/x_D$ , as illustrated for  $Pe = 0.625$  in Fig. 6. This behavior may be deduced from the previous discussion of controlling parameters.

Apparent from the trends exhibited in Figs. 3–6 is the enhanced sensitivity of the system to increased real penetration rate or increased magnitudes of Peclet number resulting from the increased penetration rate. This increased sensitivity occurs, however, with a decrease in resolution in terms of absolute tem-

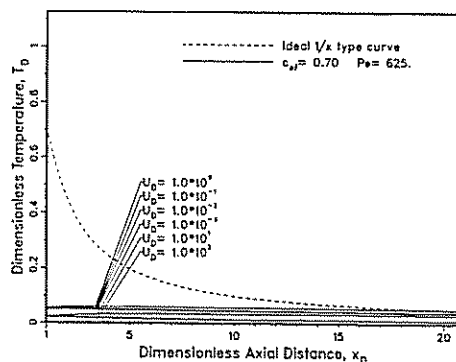


FIG. 3. Axial temperature distribution for a moving thermal source. Dynamic steady state.

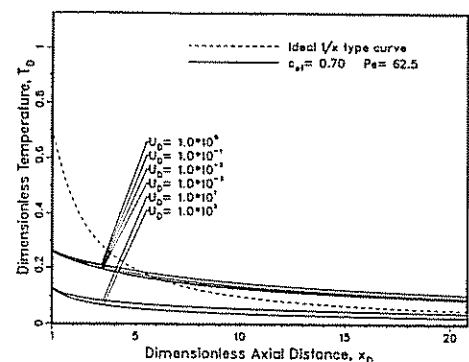


FIG. 4. Axial temperature distribution for a moving thermal source. Dynamic steady state.

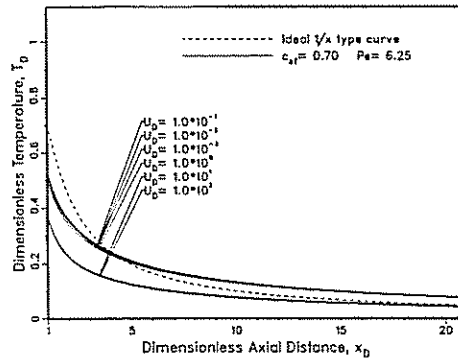


FIG. 5. Axial temperature distribution for a moving thermal source. Dynamic steady state.

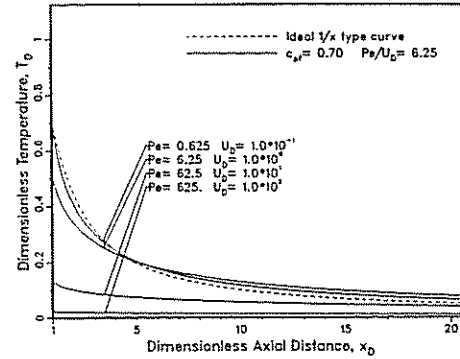


FIG. 7. Axial temperature distribution for variable rate penetration in a porous saturated medium  $C = 1.78 \times 10^{-6} \text{ m}^2 \text{ s}^{-1}$ ,  $\rho_r c_r = 2.08 \times 10^{-6} \text{ W s m}^{-3} \text{ K}^{-1}$ ,  $\rho_r c_r = 4.2 \times 10^6 \text{ W s m}^{-3} \text{ K}^{-1}$ ,  $D_s = 2.4 \text{ W m}^{-1} \text{ K}^{-1}$ ,  $D_r = 0.57 \text{ W m}^{-1} \text{ K}^{-1}$ ,  $\phi = 0.4$ .

perature magnitude. Potentially, therefore, variable penetration rates may be used to enable unambiguous determination of  $U_D$  magnitude from both temperature distribution and temperature magnitude. This possibility is exhibited in Fig. 7 where variable rate penetration in a medium of constant consolidation coefficient,  $C$ , is illustrated. Consequently, increasing real penetration rate proportionately increases both Peclet number,  $Pe$ , and dimensionless penetration rate,  $U_D$ . Penetration rates spanning  $2 \times 10^{-5} < U < 2 \times 10^{-2} \text{ m s}^{-1}$  ( $0.1 < U_D < 100$ ; and  $0.625 < Pe < 625$ ) are used to illustrate the differing responses. The lowest penetration rate elicits the diffusive response while increased penetration rates reduce the absolute magnitude of induced dimensionless temperatures. The influence of advective transport as penetration rate is increased is clearly evident in the flat temperature distribution.

In all applications so far it has been assumed that the thermal term  $\rho_r c_r / D_r$  may be determined 'a priori'. Although the component thermal conductivities and capacities are narrowly bounded, porosity ( $\phi$ ) is unlikely to be known in advance. The result of changing porosity between the extremes of 0.10 and 0.40 is illustrated in Fig. 8 for  $U_D = 1.0$  and  $U r_0 = 3.56 \times 10^{-5} \text{ m}^2 \text{ s}^{-1}$ . This corresponds to Peclet

numbers of 36.8 and 62.5. Importantly, the recorded temperature differential is large and may enable porosity to be determined if the consolidation coefficient,  $C$ , could be determined by some independent means. Fortunately, the consolidation coefficient may be determined from the hydraulic response alone [10, 11] provided the rate of pore pressure dissipation is recorded at penetration arrest. Consequently, porosity of the porous medium could be evaluated independently, through curve fitting, to enable independent appraisal of this important parameter affecting advective heat or mass transfer. This is important if parameters in addition to the consolidation coefficient are desired from penetrometer tests.

From transient analysis, temperature build up may be determined for a variety of shaft locations. For a standard penetration rate  $U r_0 = 3.56 \times 10^{-4} \text{ m s}^{-1}$  in the same porous medium ( $Pe = 625$ ) and  $U_D = 1.0$  the time history at increasing distances from the tip are illustrated in Fig. 9. Locations closest to the tip react most quickly in attaining a steady state. In real time, the equilibration is within 5 s of initiating penetration for the closest location ( $x_D = 1.14$ ;  $x = 2.03 \times 10^{-2} \text{ m}$ ). For decreased real penetration

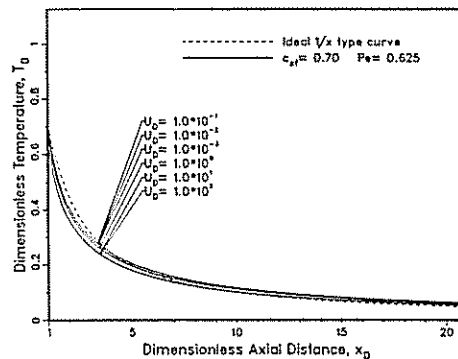


FIG. 6. Axial temperature distribution for a moving thermal source. Dynamic steady state.

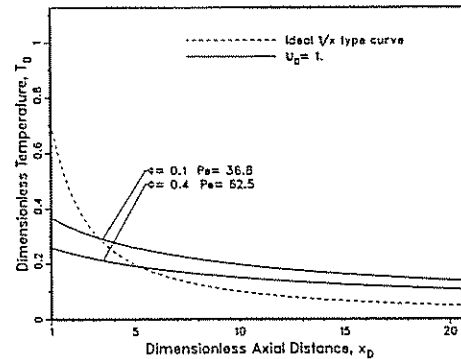


FIG. 8. Axial temperature distribution for different system porosities,  $\phi$ .  $U_D = 1$ ,  $\phi = 0.1, 0.4$ .

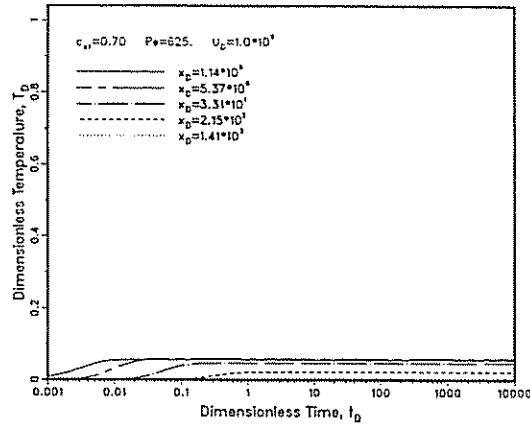


FIG. 9. Temporal response along shaft ( $x_D > 0$ ) for penetration at a standard rate of  $U = 2 \times 10^{-2} \text{ m s}^{-1}$ .

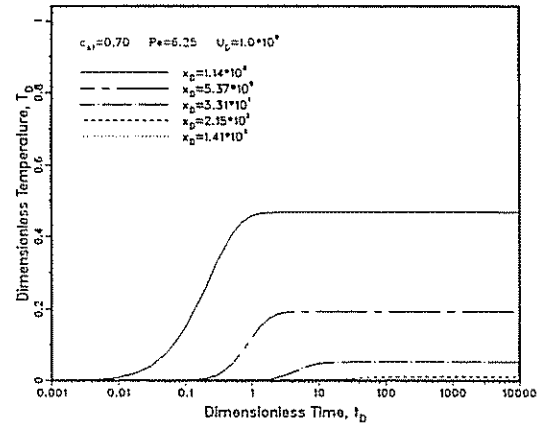


FIG. 11. Temporal response along shaft ( $x_D > 0$ ) for increased penetration rate.

rate  $Ur_0 = 3.56 \times 10^{-6} \text{ m s}^{-1}$  ( $Pe = 62.5$  and  $6.25$ ) in the same medium, as illustrated in Figs. 10 and 11, the temporal response is slowed considerably.

#### 4. CONCLUSIONS

Advective thermal dissipation around the tip of an advancing penetrometer may be measured as an index describing the consolidation and transport characteristics of the surrounding porous medium. For a static penetrometer where the flow field is insignificant the radial and axial temperatures ( $T_D$ ) conform to  $T_D = 1/R_D$ . This thermal pattern is modified by advection around the moving penetrometer allowing a series of type curves to be constructed. The groups of controlling variables are the Peclet number,  $Pe = Ur_0/\kappa_1$ , a dimensionless penetration rate,  $U_D = Ur_0/2C$ , incorporating the permeability and compressibility of the porous medium and the ratio of specific heat capacities of the porous medium and

fluid,  $c_{ef} = \rho_1 c_1 / \rho_f c_f$ . The thermal signature, measured axially along the penetrometer shaft, may be used to directly evaluate the advective thermal diffusivity if elastic compressibility of the porous medium is known or alternatively to evaluate the elastic compressibility if permeability is known. This contention follows directly from Fig. 7 where  $Pe$  is very narrowly defined through the thermal diffusivity of the saturated medium,  $\kappa_1$ . Thus, the consolidation coefficient,  $C$ , may be determined, uniquely, from curve matching to define  $U_D$ . This suggests that the hydraulic parameter,  $C$ , may be determined from this analysis without recourse to the complex and time consuming dissipation tests usually conducted in penetrometer sounding. Alternatively, since  $U_D$  is available from the pressure transient record [11] the quantity  $\rho_f c_f / D_1$  may be determined directly. This may be used to evaluate thermal transport through the corollary of equation (1) or estimate the magnitude of porosity in the porous medium as it influences rates of advective mass transfer as a close analog to heat transfer.

The real penetration rate,  $U$ , controls the sensitivity of the temperature distribution,  $T_D$ , to changes in the controlling parameters  $Pe = Ur_0/\kappa_1$  and  $U_D = Ur_0/2C$ . Two factors are of interest in determining the sensitivity of the technique to changes in the advective thermal characteristics of the porous medium. The first is the range of dimensionless penetration rates,  $U_D$ , that result in a discernible and specific thermal profile along the penetrometer shaft and the second is the distribution within that sensitive range. Threshold steady temperature distributions are apparent at both low and high values of  $U_D$ , representing the advective flux through the inversely proportional magnitude of permeability. At high penetration rates ( $Pe = 62.5$ ) the threshold behaviors are apparent at penetration rates of  $10^{-2} < U_D < 10^2$  and with decreased real penetration rate ( $Pe = 6.25$ ) this span is reduced to  $10^0 < U_D < 10^1$ . Thus, for decreased penetration rate the range sensitivity of the

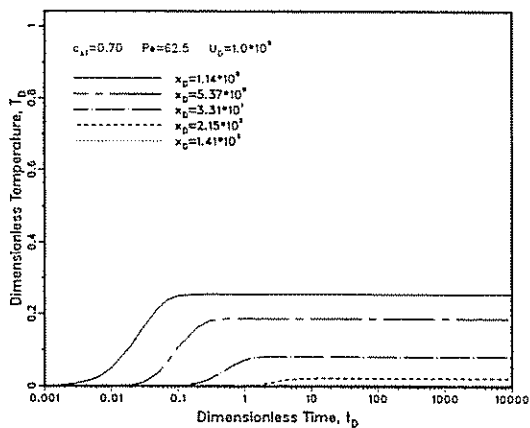


FIG. 10. Temporal response along shaft ( $x_D > 0$ ) for reduced penetration rate.

technique to permeability through the parameter  $U_D$  is correspondingly reduced. This finding may be interpreted as evidence of a decreased dependence on advective transport as a decrease in real penetration rate decreases the magnitude of the penetration induced fluid flux field.

The second factor of interest is the range of dimensionless temperatures,  $T_D$ , that result within the sensitivity range of  $U_D$ . Comparing Figs. 3 and 5, the temperature range increases with a decrease in real penetration rate or Peclet number,  $Pe$ , although the discernible range of  $U_D$  has been reduced, as noted above. As the penetration rate reduces further that the fluid flux field becomes insignificant ( $Pe = 0.625$ ) the behavior is near purely diffusive and no evaluation of the hydraulic properties is possible in the absence of an advective flux. It is therefore of considerable importance to conduct tests in a suitable range of Peclet numbers,  $Pe$ , if advective parameters are to be discerned. Penetration rate may be varied to ensure that induced advective fluxes are sufficient to cause a resolvable axial temperature change and enable characterization of the penetrated medium. The procedure therefore represents a powerful potential technique in evaluating the advective transport characteristics of unconsolidated porous media.

*Acknowledgements*—The support of the Waterloo Centre for Groundwater Research is gratefully acknowledged.

## REFERENCES

1. J. P. Carter, J. R. Booker and S. K. Yeung, Cavity expansion in cohesive-frictional soils, *Geotechnique* 36(3), 349–358 (1986).
2. A. Drescher and M. Kang, Kinematic approach to limit load for steady penetration in rigid-plastic soils, *Geotechnique* 37(3), 233–246 (1984).
3. Y. B. Acar and M. T. Tumay, Strain field around cones in steady penetration, *J. Geotech. Engng. ASCE* 112, 207–213 (1986).
4. M. M. Baligh, Strain path method, *J. Geotech. Engng. ASCE* 111(9), 1108–1136 (1985).
5. N. Janbu and K. Senneset, Effective stress interpretation of *in situ* static penetration tests, *Proc. European Symp. on Penetration Testing*, Stockholm, Vol. 1 (1974).
6. G. A. Jones and D. J. A. Van Zyl, The piezometer probe—a useful investigation tool, *Proc. 10th ICSMFE*, Stockholm, Vol. 2, pp. 489–496 (1981).
7. R. G. Campanella, D. Gillespie and P. K. Robertson, Pore pressure during cone penetration, *Proc. 2nd European Symp. on Penetration Testing*, Amsterdam, pp. 507–512 (1982).
8. M. M. Baligh and J.-N. Levadoux, Consolidation after undrained piezocone penetration. II: interpretation, *J. Geotech. Engng. ASCE* 112(7), 727–746 (1982).
9. M. T. Tumay, Y. B. Acar, M. H. Cekirge and N. Ramesh, Flow field around cone in steady penetration, *J. Geotech. Engng. ASCE* 111, 193–204 (1985).
10. J.-N. Levadoux and M. M. Baligh, Consolidation after undrained piezocone penetration. I: prediction, *J. Geotech. Engng. ASCE* 112(7), 707–726 (1986).
11. D. Elsworth, Dislocation analysis of penetration in saturated porous media, *J. Engng Mech., ASCE* 117(2), 391–408 (1991).
12. H. S. Carslaw and J. C. Jaeger, *Conduction of Heat in Solids*, 2nd Edn. Clarendon Press, Oxford (1959).

## TRANSFERT DE CHALEUR ET DE MASSE AUTOUR D'UN PENETROMETRE AVANCANT

**Résumé**—La mesure du champ de température développé autour de la pointe chaude d'un pénétromètre est proposée comme méthode de détermination des caractéristiques d'écoulement et de transport *in situ* d'un milieu poreux saturé. Le champ thermique purement diffusif développé autour d'un pénétromètre statique est modifié en présence des flux advectifs induits par la pénétration. La modification est conditionnée par la diffusivité thermique advective et la compressibilité élastique du milieu poreux, ce qui permet l'évaluation de la diffusivité de formation quand la compressibilité peut être déterminée indépendamment à partir de la variation de pression.

## WÄRME- UND STOFFTRANSPORT IN DER UMGEBUNG EINES EINDRINGENDEN HÄRTEMESSERS

**Zusammenfassung**—Es wird eine Methode zur Messung des direkten Wärmestroms und der Transportcharakteristik an einem unverdichteten, gesättigten, porösen Medium vorgeschlagen. Sie basiert auf der Messung des Temperaturfeldes, das von der beheizten Meßspitze eines Härtemessers ausgeht. Das Temperaturfeld in der Umgebung einer ruhenden Prüfspitze wird durch die von der eindringenden Prüfspitze verursachten horizontalen Wärmeströme verändert. Die Veränderung ist durch die horizontale Temperaturleitfähigkeit und die elastische Verformung des porösen Mediums gekennzeichnet. Damit wird es möglich, die Temperaturleitfähigkeit einer Schicht zu bestimmen und gleichzeitig die Kompressibilität aus dem zeitlichen Druckverlauf zu ermitteln.

## ТЕПЛО- И МАССОПЕРЕНОС ВОКРУГ ДВИЖУЩЕГОСЯ ПЕНЕТРОМЕТРА

**Аннотация**—Измерение теплового поля, развивающегося вокруг нагретого конца пенетрометра, предложено в качестве метода определения характеристик течения и переноса для рыхлых насыщенных пористых сред. При наличии адвективных потоков за счет теплопроводности происходит модификация чисто теплового поля, образующегося вокруг статического пенетрометра. Это изменение обусловлено адвективной температуропроводностью и упругой сжимаемостью пористой среды, что позволяет оценивать температуропроводность среды вокруг пенетрометра в случае, когда сжимаемость можно определить независимо по регистрации изменения давления.